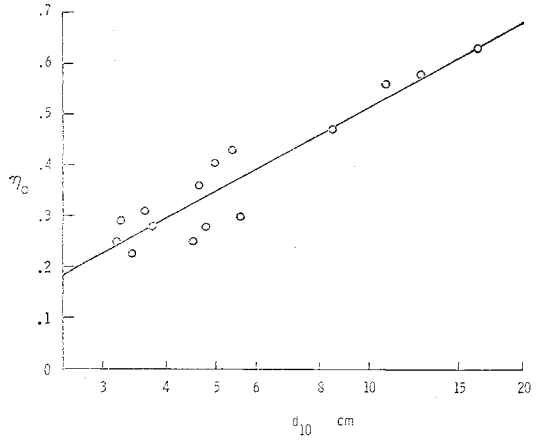

Fig. 3 Over-all efficiency as a function of the characteristic length for decrease of propellant density by a factor of ten, (d_{10}), A7 and A8 electrodes, and 220 μf capacitance were used with a variety of valves.

the increased capacitance extending the discharge period to match the ion acceleration time, or the increased propellant flow rate increasing propellant availability as shown on Fig. 1, also contributed. Measurement techniques and basic accelerator design have been covered in detail elsewhere and so will not be reported here.

Despite optimal settings of all gross parameters, wide variations in performance, discharge current wave forms, and even visual appearance of the discharge could still be observed. While a wide variety of factors play some role in this, a strong correlation of accelerator over-all efficiency with the prefire propellant distribution supports the view that the details of valve design are dominant.

The axial propellant density gradients were the specific characteristics studied and it was found that the more gentle these were, the higher the resulting efficiency. Figure 3 shows the over-all efficiency at 5000 sec specific impulse as a function of the characteristic distance over which the axial propellant density would decrease by a factor of ten (d_{10}). These data were obtained by standard fast ionization gage techniques with a wide variety of valve designs.

The combined requirements of gentle gradients and a high available propellant fraction η_m' can be interpreted as support for a short propellant pulse with a width comparable to the active length of the accelerator. Accelerator triggering can then be timed to occur when the density peak has propagated to a position midway between the electrodes and spread so that the gradients are small. The best performance has been obtained with just such a propellant distribution.

The validity of the measurements leading to this high performance has been supported by independent measurements. The specific impulse determined from thrust and mass flow has been validated by electrostatic gridded probe analyses. The values found by either method were essentially the same. The over-all efficiency itself was obtained from the calorimetric efficiency, the propellant mass utilization and the ion velocity distribution as well as the more conventional thrust, mass flow, and power input determination. The values determined in this way differed by about 6%, well within the uncertainty of the individual measurements.

Correlation of Propellant Density Gradients and Capacitance with the Efficiency of a Plasma Gun

C. S. Cook,* P. Gloersen,† B. Gorowitz,‡ and T. W. Karras§
General Electric Space Sciences Laboratory, King of Prussia, Pa.

Additional studies have been made of a repetitively pulsed coaxial plasma gun. Gross performance characteristics were found to depend most heavily on axial propellant density gradients and circuit capacitance; and over-all efficiency averaged over many runs was higher than that previously reported, i.e., about 60% at 5000 sec specific impulse. Diagnostic techniques were applied to the gun; the data were used to corroborate the gross performance measurements and to help understand differences in operation.

I. Introduction

CONSIDERABLE effort has been applied towards improvement of the performance of coaxial plasma accelerators with regard to those characteristics deemed important for eventual application to space flight.[1–10] Some of the more recent results are reported here. As support for this work, there has also been a concerted effort at understanding the acceleration processes through the use of detailed diagnostics. The results of some of these techniques have been discussed separately in varying degrees elsewhere[2–12]; however, additional information and interpretations have become available and are also included here.

The earliest systematic studies directed toward improving the performance of these devices used exhaust stream calorimetry for monitoring the trends as accelerator electrode shape, discharge circuit parameters, and mass loading techniques were changed.[5] Later studies made use of mass flow measurements, input power measurements, and a thrust balance on which the accelerator was mounted.[6] In both these studies, successive design changes resulted in a continuing increase in the efficiency of the plasma gun to the point where long-term runs and detailed diagnostics became warranted in order to confirm the measurements obtained by the earlier techniques. After an extended period of successful

Received July 14, 1969; revision received January 19, 1970. We wish to acknowledge useful discussions with our colleague F. W. Mezger.

* Research Engineer, Laser Applications.
† Consulting Scientist, Experimental Physics. Associate Fellow AIAA.
‡ Research Chemist, Structural Materials Programs. Member AIAA.
§ Principal Scientist, Plasma Physics. Member AIAA.

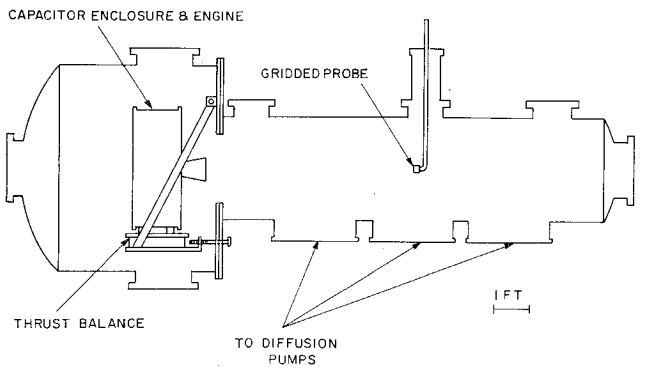

Fig. 1 Outline of plasma accelerator test facility.

testing during which this was done, variations in the operating characteristics of the coaxial accelerator became apparent, as reflected in lower levels of performance than had been experienced previously.[10] Diagnostic studies were also made during this period, making possible a comparison of the different characteristics of operation.

The appearance of differences in operation resulting from identical gross settings of mass flow, voltages, and capacitance emphasizes the importance of understanding the detailed processes affecting accelerator operation. The diagnostic measurements summarized here are necessary for such an understanding.

II. Experimental Arrangements

Details of the experimental techniques employed have been described in various other papers.[6-8] Briefly, the coaxial gun and its energy storage system are mounted on a sensitive thrust balance in a large high vacuum test chamber (Fig. 1). A major new convenience that has been added is a variable capacitance energy storage unit (Fig. 2). Background pressures during 10 Hz repetitive operation of the gun were typically in the 10^{-6}–10^{-5} mm range. Propellant mass flows were determined in several ways, including calibrated ball and tapered tube flowmeters, rate of change of a calibrated volume at constant pressure, and flow transducers. Careful attention to monitoring the temperature and pressure at all points in the propellant feed system was required. Power inputs were obtained from measurements of capacitor voltages just prior to and immediately after each discharge, measurements of the capacitance and capacitor Q, and a determination of the pulsing rate. To complete the set of gross performance measuring techniques, a large water-cooled calorimeter was used to capture the exhaust stream in order to determine its power content. This latter measurement is not considered to be as reliable as the others since it is known that mass flow patterns in the vicinity of the gun were changed with the calorimeter in place, and occasional changes in the thrust balance reading for externally equivalent operating conditions were observed.

Contrary to the preceding measuring techniques, the plasma diagnostics were carried out on a single-shot basis. Since large variations in gun performance have been noted when changing from an occasional single-shot operation to one of steady-state repetitive running,[5] considerable care was exercised in properly preconditioning the gun by repetitive firing just prior to the single shot required for the diagnostics data. In addition, the shot-to-shot repeatability was monitored. These procedures applied to the B_θ probe, the multigridded particle probe,[8] the vacuum ultraviolet (VUV) spectrometer,[12] and the Langmuir probe measurements.

III. High-Efficiency Performance Characteristics

One of the changes in the performance of the repetitively-pulsed plasma accelerator[6] came as an indirect result of increasing the energy storage capacitance, as illustrated in Fig. 3. It can be seen that the over-all efficiency, $\eta_0 = T^2/2\dot{m}P(1 - 1/Q)$, at a given specific impulse was about doubled when the capacitance was quadrupled. Here, T is the average thrust, $\dot{m}$ is the average input mass flow, P is the average input power and Q is the quality factor of the capacitor. Such a significant change in performance as a result of capacitance change might at first be thought to be the sole result of tuning the capacitance to particle residence time within the gun. It should be pointed out that the peak current, and hence the coupling, was not increased with the increase in capacitance because the voltage was lowered to keep the energy constant. Although such circuit considerations govern to some extent, it is felt that the most important contribution to the improved performance resulted from the higher mass loading at a given energy-per-shot value permitted by lowering the voltage while increasing the capacitance. The higher permissible mass loading, in turn, gave rise to three distinct improvements in operating conditions. 1) A more gentle axial propellant density gradient (see Sec. V for the consequences of this) was obtained because of the different valve and nozzle condi-

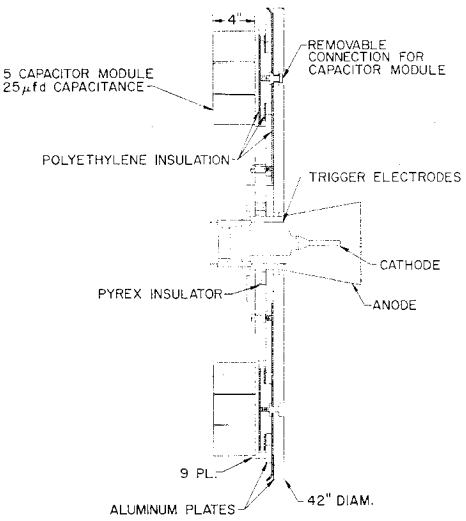

Fig. 2 Thruster assembly showing variable capacitance energy storage.

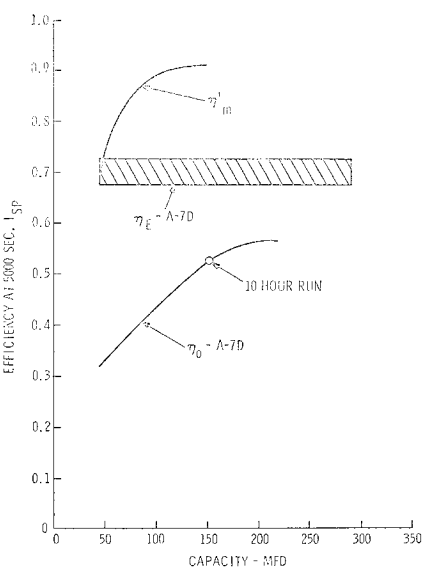

Fig. 3 Available mass fraction n_m', fraction of input energy collected in a downstream calorimeter n_E, and over-all efficiency η_o, at operating conditions resulting in a specific impulse of 5000 sec as functions of the capacitance of the energy storage bank. These data were obtained with low axial propellant density gradients.

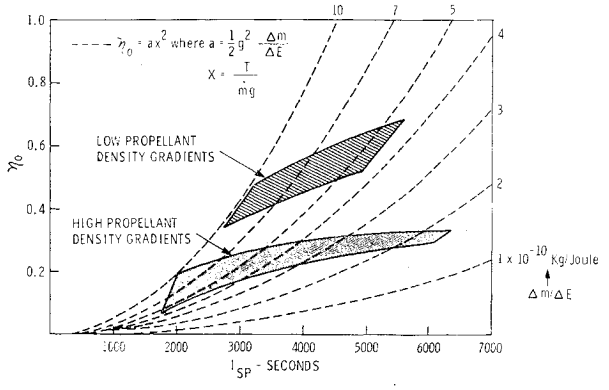

Fig. 4 Illustration of the variable operation of the A-7XD accelerator. The two bands represent operating extremes observed in the same A-7XD configuration having changed only the characteristics of the propellant inlet valve.

tions at the increased mass flow rates. 2) A higher fraction of the injected mass was available to the discharge,[7] as indicated by the η_m' curve of Fig. 3, due to a more favorable operating condition for the valve at the higher mass flow rates.[7,10] (See also Sec. V.) 3) Higher values of $\Delta m/\Delta E$, the mass per unit discharge energy, were also obtained at a given I_{sp}. As can be seen in Fig. 4, this is equivalent to a higher over-all efficiency at a given I_{sp}.

According to the exhaust stream calorimetry, there was little or no change in the transfer efficiency of electrical energy to total stream energy during these changes, as indicated by the η_E curve of Fig. 3. The additional increase in η_0 must then be attributed to either a higher mass utilization factor during the discharge or a higher velocity efficiency,[13] or both.

There was a great deal of support for the validity of these performance measurements. They were obtained for extended periods at many different times and under a variety of conditions. Particularly noteworthy in this regard is the 10 hr run at a pulsing rate of 5 sec^{-1} with the performance figures indicated in Fig. 3. Corroboration of this performance was obtained with the gridded probe and calorimeter and will be discussed in a succeeding section.

IV. Discussion of Performance Variations

Variation of the performance as a function of the specific impulse, $I_{sp} = T/\dot{m}g$, is shown in Fig. 4. Superimposed on the performance data are curves of constant mass per unit discharge energy. These are parabolae since

$$\eta_0 = a\,(T/\dot{m}g)^2 \text{ where } a = \tfrac{1}{2}\,g^2\Delta m/\Delta E \qquad (1)$$

The purpose of the curves is to demonstrate that a given gun loading, i.e., a given "a" as defined in Eq. (1), can give rise to a wide range of performance values, depending on the discharge conditions obtained in the gun. A very pointed demonstration of this is the change of operation experienced in the same A-7XD accelerator when the valve construction was altered[10] as indicated by the two extreme bands in Fig. 4.

The basic symptoms of low-efficiency operation are always the same. Sensitivity to parametric changes is greatly reduced.[10] For instance, variation of the triggering delay rarely shows a clear-cut optimum in contrast with the marked maximum found at higher efficiency.[6] Alterations in propellant,[6] electrode length[5] and capacitance show only small effects while in high-efficiency operation they are all large. Differences in the current and voltage waveforms, as illustrated in Fig. 5, are also observed. In addition, the visual appearance of the exhaust plume is altered. High-efficiency performance is typified by a bright central core region about 2 cm in diameter and several centimeters in length attached to the central electrode; low efficiencies are typified by a more diffuse discharge. Evidently, the discharge does not develop properly in low-efficiency operation.

It should be mentioned that when speaking of impedance-matching to the external circuitry, the current waveforms (see Fig. 5, for instance) have been nonsinusoidal and near the critical damping point over a wide variety of flow and capacitance conditions. Thus proper circuit matching has been realized over most of the experimental conditions encountered here. On the other hand, small changes in the current waveform (Fig. 5) have been associated with wide variations in the performance, indicative of a multitude of plasma characteristics giving rise to good circuit matching, not all of them leading to good performance.

Although a variety of factors undoubtedly play some role in causing this, a strong correlation of accelerator over-all efficiency with the prefire propellant distribution supports the view that valve design is dominant. The presence of very small quantities of pump oil vapor (partial pressure of less than 10^{-7} mm) or background gas (partial pressure less than 10^{-5} mm) have an effect upon triggering and far downstream characteristics, but no effect upon engine performance such as that of propellant distribution.

In this context, it is important to emphasize the ineffectiveness of impurity addition. Even in the extreme case when oil was spread on the electrodes, only a three percentage point increase in efficiency was observed at 5000 sec specific impulse. The only consistent and significant effect of oil contamination was that stable triggering could be obtained with a factor of two less mass flow.[10]

V. Internal Diagnostics

Two kinds of measurements were made within the gun to establish conditions immediately before and during the discharge; measurements of propellant distribution and azimuthal magnetic field (B_θ).

The technique, and many of the results of using a fast response ionization pressure gage for predischarge mass distribution studies within the gun barrels, have been discussed in detail elsewhere.[7] Only the differences noted in these gas density distributions for various operating conditions will be discussed here.

Differentiation between conditions resulting in various efficiencies can be most effectively made by consideration of the fraction of the injected propellant which is within the gun. The importance of the first factor has been emphasized previously[7,10] and it will suffice here to summarize by pointing out that a large fraction of the injected propellant must be in the interelectrode space at the time of accelerator triggering. Valve bounce and long propellant flow times are the main cause of low propellant availability.

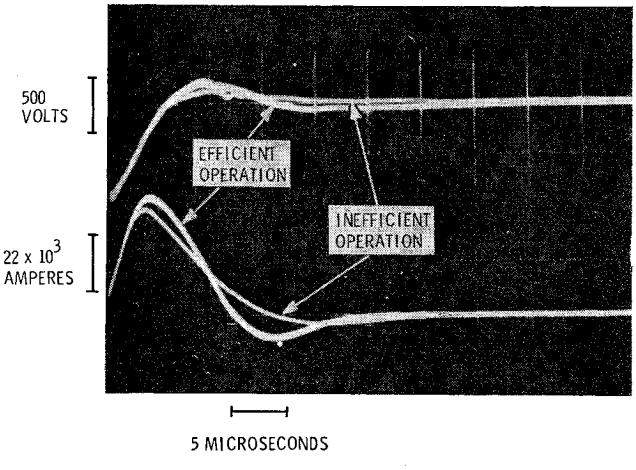

Fig. 5 Discharge waveforms for the A-7XD accelerator.

The question of gradients in the prefire propellant distribution, on the other hand, has not been given much attention. Qualitative judgements have been made that a slowly varying axial propellant density distribution is superior to a bunching of the propellant in a single "slug."[7] The reverse analysis supporting increasing efficiency with more sharply decreasing densities along the axis also can be found,[14] but it assumes that a largely radial, compressed current distribution (snowplow) can be formed in the discharge chamber. However, such discharge characteristics were not obtained in these experiments.

Assembly of a large quantity of data gives support to the former view. Figure 6 shows a monotonic relation between the characteristic distance over which the axial propellant density would decrease exponentially by a factor of ten (d_{10}) and the over-all efficiency of the accelerator at 5000 sec. These data points represent a wide variety of valve designs and triggering schemes operating within similar electrode configurations.[10] The capacitance and other electrical and mechanical characteristics were very close to those used earlier.

This figure should not be taken as support of a uniformly filled accelerator with propellant extending far beyond the interelectrode region. The best performance was obtained when a distinct propellant pressure peak existed somewhere within the interelectrode volume while very little gas had passed beyond the accelerator muzzle. Figure 6 can be interpreted as support for very short propellant pulses with triggering designed to occur when the density peak has propagated to a position midway between the electrodes and spread so that the gradients are small. In this way, the requirements of a large available propellant fraction and gentle axial density gradients can be met simultaneously. Other details of the propellant distribution, such as the gas density near the trigger wires, are important but none seem to be as strongly correlated with over-all efficiency as the two factors mentioned above.

The azimuthal magnetic field (B_θ) was determined during the discharge with a small multiturn search coil. While some of these B_θ probe data were obtained during high efficiency operation, they were in insufficient detail to permit meaningful comparisons. Much more detailed data were obtained during low-efficiency runs;[10] and they are plotted in the form of rB_θ contours in the r, z plane in Fig. 7. Superimposed upon these contours are the isobars deduced from the fast pressure probe data taken under similar initial conditions prior to the discharge. It will be noted that because of the steep axial density gradient, the bulk of the current distribution near current maximum terminates in the region of the gas outlet nozzles where the value of the inductance per unit length L' has not reached its highest values. If one expresses the instantaneous axial force developed in the gun in terms of the total discharge current, i (t), and an average inductance per unit length, $\overline{L'}$, the axial force is given by $\frac{1}{2}\overline{L'}\overline{i^2}$. In the A-7XD gun, $\overline{L'}$ is a function of the current distribution in the discharge. It is believed that during high efficiency operation, the bulk of the current at current maximum terminated nearer the region around the tip of the inner electrode, giving rise to a higher $\overline{L'}$, and therefore a higher peak axial force for a given peak discharge current. Some support

Table 1 Comparison of efficiency factors

	Axial propellant density gradients	
	Low	High
η_0 at 5000 secs	$\sim$ 60%	$<$ 30%
η_E	$\sim$ 70%	$\sim$ 50%
$\eta_{v/\cos\alpha}$	$\sim$ 87%	$\sim$ 70%
η_p	$\sim$100%	$\sim$100%
η_m'	$\sim$ 90%	$\sim$ 64%

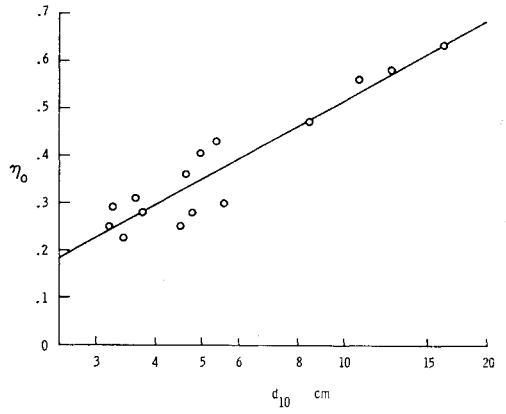

Fig. 6 Over-all efficiency as a function of the characteristic length for decrease of propellant density by a factor of ten, (d_{10}), A7 and A8 electrodes, and 220 μf capacitance were used with a variety of valves.

for this hypothesis comes from the visual observation of a bright central core in the discharge beyond the muzzle during high-efficiency operation, as mentioned earlier. Perhaps an even more important contribution to poor performance is the large component of radial force developed as a result of the extensive axial component of the discharge current distribution near current maximum shown in Fig. 7.

These arguments are consistent with some presented earlier[5] on the basis of circuit impedances, provided that the factor dL/dt is not assumed to be given by L' (t) dx/dt, where x (t) is the position of a well-defined mass slug. Such an assumption requires the movement of a well-defined current sheet and accompanying mass, which have not been observed in these experiments.

There is another viewpoint, however, which is not necessarily dependent on a time-variation of L (t) as seen in the gun terminals, but that arises from considering a conducting medium moving across fixed magnetic field lines. This phenomenon has been analyzed[16] in terms of a manifold of current microsheets, each attached to a slug of particles beginning at the breech of the gun and following that slug to the muzzle. Thus, the slug model, involving dL $(t)/dt$, pertains to each microsheet, but the integrated effect over-all microsheets may lead to a steady-state inductance. This view is important for interpreting the experimental results obtained here when the current distribution is not changing rapidly, yet the potential across the discharge is still high.

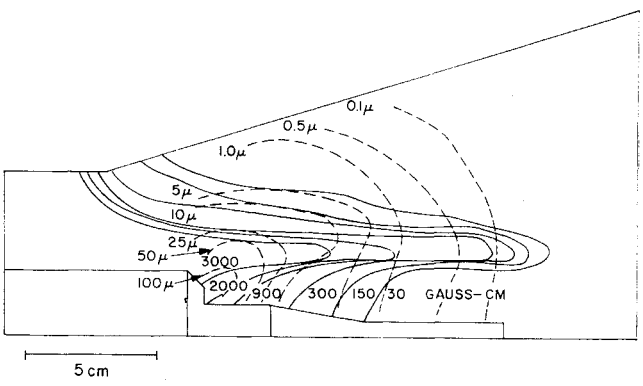

Fig. 7 Data from fast-response pressure and magnetic field probes for the higher propellant density gradient case. Pressure probe data (dashed curves) are given in units of microns for a time corresponding to discharge initiation about 450 μsec after actuation of the pulsed gas valve. The solid curves represent the product rB_θ in units of gauss-cm and corresponding to a time near current maximum 2 μsecs after initiation of the discharge. See Ref. 10 for design details of the thruster.

It is, of course, central to the understanding of steady-state devices such as the MPD arc.

Verifying either viewpoint by relating an integrated current distribution to mechanical motion would require more B_θ probe data than are now available. Detailed knowledge of the prefire propellant density distribution would also be needed along with relevant thrust and downstream probe data. Such a series of measurements has not yet been performed.

VI. Downstream Diagnostics

Extensive diagnostic measurements were made downstream from the accelerator in order to corroborate the performance constructed from the thrust and mass flow.

Power efficiency (η_E) measurements with a calorimeter were performed as in the past.[5] Values of about 70% were obtained during optimum conditions and about 52% for a typical run with steep prefire axial propellant gradients. Calorimetric measurements made elsewhere[15] with a slightly different accelerator, also showed up to 72%, supporting the view that such high efficiencies can be reproduced with similar but not identical equipment.

The specific impulse, given earlier by $T/\dot{m}g$, was also obtained from the average exhaust velocity (v/g) determined from multigridded particle probe data.[8] Thus, two independent determinations were made.

Similarly, the over-all efficiency was expressed in two ways[13]

$$\eta_0 = T^2/2\dot{m}P \tag{2}$$

and

$$\eta_0 = \eta_E \eta_m \eta_v \tag{3}$$

where

$$\eta_v = (\bar{v}^2/\overline{v^2})\ \overline{\cos^2\alpha} \tag{4}$$

assuming that the velocity distribution did not change with spreading angle α as was the case in these experiments; and η_m, the mass utilization efficiency, is composed of the two factors η'_m, the available mass fraction and η_p, the fraction of the propellant in the chamber at the onset of the discharge that is accelerated. If the thrust is mostly due to the accelerated particles of average velocity $\overline{v_{\text{ion}}}$,

$$T \approx (\eta_m' \eta_p \dot{m})\ \overline{v_{\text{ion}}} \tag{5}$$

and an indication of the value of η_p can be obtained from the experimentally determined values of T, η_m', $\dot{m}$, and $\overline{v_{\text{ion}}}$.

The multigridded particle probe[8] was used to obtain the required ion velocity distribution data across the entire cross-section of the accelerated plasma beam. Data were obtained for both extremes in efficiency, but only the data obtained during high performance were adequate to permit determination of total velocity distribution functions.

The most detailed data were obtained for operating conditions similar to that of the 10 hr run indicated in Fig. 3. The distribution function was determined at four different points in the exhaust stream, one of which was on axis and another of which was in the edge of the beam where the signals were an order of magnitude smaller than elsewhere. As has been noted previously,[8] the average velocity of the accelerated ions obtained under these conditions was about 5.2×10^4 m/sec across the entire cross section of the beam. Computations of η_p from Eq. (5) yielded a value of 95%, indicating essentially complete utilization of the available gas. Thus, in Eq. (3), η_m' can be substituted for η_m to a good approximation.

The distribution function was also used to obtain the quantities $\bar{v}^2$ and $\overline{v^{-2}}$, the first and second components of η_v'. The third, $\overline{\cos^2\alpha}$, was determined by forming a radial density distribution function from the integrated velocity distributions at a number of different radial positions across the beam. The three quantities were combined to form the ion velocity efficiency $\eta_v = 0.85$. The value of the over-all efficiency was then found in two independent ways from Eq. (2) and (3)

$$\eta_0 = (\eta_E)\ (\eta_m)\ (\eta_v)$$
$$= (0.70)\ (0.90)\ (0.85) = 0.53$$

and

$$\eta_0 = T^2/2\dot{m}P = 0.50$$

which agree well within the uncertainty of the measurements and thus strongly support their validity.

A similar comparison could not be made for low-performance operation because of the lack of gridded probe measurements off the beam axis. Limited measurements near the axis indicated that the beam had a wider spread in velocities, $\bar{v}^2/\overline{v^2} \sim 0.7$, and a greater divergence. Combined with the reduced calorimetric efficiency ($\sim$52%), this tended further to support the view that steepening of the axial propellant gradient produced a significant change in the discharge, its current distribution, and acceleration characteristics.

To clarify this picture further, a vacuum ultraviolet (VUV) spectrometer and a windowless source of xenon lines used as a background illuminator were combined to obtain particle densities and velocities by a VUV absorption technique.[12] Unfortunately, this technique was not available during high-efficiency operation of the gun so that such data are not available for those conditions. For those conditions where it could be used, a combination of light source characteristics and low ion densities limited absorption so that only the xenon neutrals could be so monitored. A major result of these investigations[12] was the determination that about 0.25% of the particles in the exhaust were in a separate neutral component with particle energies of around 11 ev. Although the number of particles in this pulse is so low as to be unimportant in accounting for any contribution to the thrust, their presence has important implications for the discharge conditions within the gun.

The only reasonable mechanism available for the production of these neutrals is charge exchange of weakly accelerated xenon ions with an unionized background of xenon neutrals at a pressure of the order of a micron. In addition, the exchange must have occurred in a location where not only a significant number of propellant atoms could have survived unionized up to the time of exchange, but thereafter the new 11 ev neutral could have remained neutral until the discharge was over. Since a good fraction of the available propellant was within the accelerator at the time of discharge, this reasoning implies poor utilization of available propellant (low η_p) during low-performance operation. Any position in the interelectrode region with low current density but significant mass density shown in Fig. 7 is a prime candidate for this region of charge exchange and poor utilization.

Finally, in order to obtain an identification of the species involved in low efficiency operation, the VUV emission was studied spectroscopically.[12] At the same time, a Langmuir probe was placed in the exhaust stream at about the location of the optical path used for the VUV emission studies. The magnitude and time profile of probe currents obtained indicated that the VUV emission was from a moving plasma pulse. A VUV spectrogram of the gun exhaust revealed the presence of xenon atoms, singly and doubly ionized xenon, and carbon. Since hydrogen atoms also were observed to emit in this wavelength region, it is likely that protons also were present. Using the VUV instrument as a monochromator, it was found that the time contours of all the emitting species were about the same as the time contour of the Langmuir probe signal. This supports similar observations made with the multigridded probe.[8]

VII. Conclusions

High-performance operation of a coaxial gun has been demonstrated and corroborated by a variety of measuring

techniques. This corroboration has taken the form of extended runs and measurements of the performance by independent techniques. Low performance has also been observed and Table 1 lists a comparison of the pertinent efficiency factors.

High performance has correlated most strongly with large capacitance (220 μf), low voltage (1kv) and slowly varying axial propellant gradients. Factors discussed in previous papers such as a high available mass fraction,[5] optimum triggering delay time,[4] and the appropriate electrode design,[3] are essential but not sufficient for such performance..

References

[1] Gloersen, P., Gorowitz, B., and Palm, W., "Experimental Performance of a Pulsed Gas Entry Coaxial Plasma Accelerator," *ARS Journal*, Vol. 31, No. 8, Aug. 1961, pp. 1158–1161.

[2] Gooding, T. J., Hayworth, B., and Lovberg, R. H., "Instabilities in a Coaxial Plasma Gun," *AIAA Journal*, Vol. 1, No. 6, June 1963, pp. 1289–1292.

[3] Larson, A. V. et al., "An Energy Inventory in a Coaxial Plasma Accelerator Driven by a Pulse Line Energy Source," *AIAA Journal*, Vol. 3, No. 5, May 1965, pp. 977–979.

[4] Michels, C., "Analytical and Experimental Performance of Capacitor Powered Coaxial Plasma Guns," *AIAA Journal*, Vol. 4, No. 5, May 1966, pp. 823–830.

[5] Gloersen, P., Gorowitz, B., and Kenney, J. T., "Energy Efficiency Trends in a Coaxial Gun Plasma Engine System," *AIAA Journal*, Vol. 4, No. 3, March 1966, pp. 436–441.

[6] Gorowitz, B., Karras, T. W., and Gloersen, P., "Performance of an Electrically Triggered Repetitively Pulsed Coaxial Plasma Engine," *AIAA Journal*, Vol. 4, No. 6, June 1966, pp. 1027–1031.

[7] Karras, T. W., Gorowitz, B., and Gloersen, P., "Neutral Mass Density Measurements in a Repetitively Pulsed Coaxial Plasma Accelerator," *AIAA Journal*, Vol. 4, No. 8, Aug. 1966, pp. 1366–1370.

[8] Karras, T. W., Gorowitz, B., and Gloersen, P., "Experimentally Measured Velocity Distribution in the Plasma Stream of a Pulsed Coaxial Accelerator," *The Physics of Fluids*, Vol. 9, 1966, p. 1875.

[9] Ashby, D. E. T. F. et al., "Exhaust Measurements on the Plasma from a Pulsed Coaxial Gun," *AIAA Journal*, Vol. 3, No. 6, June 1965, pp. 1140–1142.

[10] Gorowitz, B. et al., "Research and Development on the Pulsed Plasma Accelerator," CR-72271, 1967, NASA.

[11] Lovberg, R. H., "Schlieren Photography of a Coaxial Accelerator Discharge," *The Physics of Fluids*, Vol. 8, 1965, p. 177.

[12] Gloersen, P., "Observation of Fast Neutrals Projected from a Coaxial Gun," *The Physics of Fluids*, Vol. 12, 1969, p. 945.

[13] Miller, D. B. and Gibbons, E. F., "Experiments with an Electron Cyclotron Resonance Plasma Accelerator," *AIAA Journal*, Vol. 2, No. 1, Jan. 1964, pp. 35–41.

[14] Black, N. A., and Jahn, R. G., "Dynamic Efficiency of Pulsed Plasma Accelerator," *AIAA Journal*, Vol. 3, No. 6, June 1965, pp. 1209–1210.

[15] Derevschikov, V. A. and Rusakov, N. V., "Angular Energy Distribution from an End Type Coaxial Electrodynamic Accelerator," *Zhurnal Tekhnicheskoi Fiziki*, Vol. 37, 1968, p. 2237; also *Soviet Physics—Technical Physics*, Vol. 12, 1968, p. 1650.

[16] Mezger, F. W., "Stationary Current Sheet Model for Plasma Acceleration," TIS R65SD21, General Electric; also Gorowitz, B., Karras, T., and Gloersen, P., "Study of Parametric Performance of a Two Stage Repetitively Pulsed Plasma Engine," CR-54846, NASA.